THE JOURNAL OF BIOLOGICAL CHEMISTRY Vol. 277, No. 41, Issue of October 11, pp. 38029–38036, 2002
Printed in U.S.A.

Inactivation of Human Peroxiredoxin I during Catalysis as the Result of the Oxidation of the Catalytic Site Cysteine to Cysteine-sulfinic Acid*

Received for publication, July 3, 2002, and in revised form, August 1, 2002
Published, JBC Papers in Press, August 2, 2002, DOI 10.1074/jbc.M206626200

Kap-Seok Yang‡, Sang Won Kang‡§, Hyun Ae Woo, Sung Chul Hwang¶, Ho Zoon Chae‖, Kanghwa Kim, and Sue Goo Rhee‡‡**

From the Laboratory of Cell Signaling, NHLBI, National Institutes of Health, Bethesda, Maryland 20892

By following peroxiredoxin I (Prx I)-dependent NADPH oxidation spectrophotometrically, we observed that Prx I activity decreased gradually with time. The decay in activity was coincident with the conversion of Prx I to a more acidic species as assessed by two-dimensional gel electrophoresis. Mass spectral analysis and studies with Cys mutants determined that this shift in pI was due to selective oxidation of the catalytic site Cys^{51}-SH to Cys^{51}-SO_2H. Thus, Cys^{51}-SOH generated as an intermediate during catalysis appeared to undergo occasional further oxidation to Cys^{51}-SO_2H, which cannot be reversed by thioredoxin. The presence of H_2O_2 alone was not sufficient to cause oxidation of Cys^{51} to Cys^{51}-SO_2H. Rather, the presence of complete catalytic components (H_2O_2, thioredoxin, thioredoxin reductase, and NADPH) was necessary, indicating that such hyperoxidation occurs only when Prx I is engaged in the catalytic cycle. Likewise, hyperoxidation of Cys^{172}/Ser^{172} mutant Prx I required not only H_2O_2, but also a catalysis-supporting thiol (dithiothreitol). Kinetic analysis of Prx I inactivation in the presence of a low steady-state level (<1 μM) of H_2O_2 indicated that Prx I was hyperoxidized at a rate of 0.072% per turnover at 30 °C. Hyperoxidation of Prx I was also detected in HeLa cells treated with H_2O_2.

Peroxiredoxins are a family of peroxidases that reduce hydrogen peroxide and alkyl hydroperoxides to water and alcohol, respectively, with the use of reducing equivalents provided by thiol-containing proteins (1–3). The first peroxiredoxin (Prx)[1] proteins to be discovered were a 25-kDa yeast protein initially called thiol-specific antioxidant enzyme (4–6), and a 21-kDa *Salmonella typhimurium* alkyl-hydroperoxide reductase termed AhpC (7–10). Subsequently, a mammalian homolog of thiol-specific antioxidant/AhpC was purified; and it, together with thiol-specific antioxidant and AhpC, defined a family of peroxidases that now includes six mammalian isoforms (Prx I–VI) and members identified in organisms from each kingdom (3, 10, 11).

All Prx proteins contain a conserved Cys residue, which corresponds to Cys^{51} in mammalian Prx I, in the N-terminal portion of the molecule (10, 11). The majority of Prx proteins, including four (Prx I–IV) of six mammalian peroxiredoxins, contain an additional conserved Cys residue in the C-terminal region that corresponds to Cys^{172} in mammalian Prx I (2, 3, 12, 13). The Prx enzymes containing two conserved Cys residues are thus called 2-Cys Prx, in comparison with a small number of Prx proteins termed 1-Cys Prx, which contain only one conserved cysteine residue in the N-terminal domain (2, 10). In 2-Cys Prx enzymes, the N-terminal conserved cysteine is oxidized by H_2O_2 to cysteine-sulfenic acid (Cys^{51}-SOH), which then reacts with Cys^{172}-SH of the other subunit to produce an intermolecular disulfide (1, 14). Reduction of the disulfide intermediate of Prx I–IV is specific in that it can be achieved by thioredoxin (Trx), but not by GSH or glutaredoxin (15, 16). Thus, the reducing equivalents for the peroxidase activity of Prx I–IV are ultimately derived from NADPH via thioredoxin reductase (TrxR) and Trx. Not all Prx enzymes containing both conserved Cys residues are reduced by Trx: the bacterial Prx AhpC is reduced by AhpF, which contains both Trx and TrxR domains (10, 17). In the absence of a physiological electron donor, the peroxidase activities of 2-Cys Prx enzymes can be supported by small thiol molecules such as dithiothreitol (DTT) and 2-mercaptoethanol, but not by GSH (1, 14, 15). In 1-Cys Prx enzymes, including mammalian Prx VI, the conserved cysteine is also the site of oxidation, but remains in a sulfenic acid state upon oxidation because there is no nearby partner cysteine to form a disulfide bond (18, 19). Trx cannot reduce this sulfenic acid-containing intermediate (18, 20). GSH has been proposed to be the electron donor, but these data remain controversial (18, 20–23).

The crystal structures of 2-Cys and 1-Cys Prx enzymes reveal that the catalytic cysteine is located in a small pocket formed by the N- and C-terminal domains of the two subunits

* This work was supported in part by Korea Research Foundation Grant KRF-2001-015-DP0482 (to H. Z. C.) and by the Korea Science and Engineering Foundation through the Center for Cell Signaling Research at Ewha Womans University, Korea (to H. A. W.). The costs of publication of this article were defrayed in part by the payment of page charges. This article must therefore be hereby marked "*advertisement*" in accordance with 18 U.S.C. Section 1734 solely to indicate this fact.

‡ Both authors contributed equally to this work.

§ Present address: Center for Cell Signaling Research and Div. of Molecular Life Sciences, Ewha Womans University, 11-1 Daehyun Dong, Seodaemoon-gu, Seoul 120-750, Korea.

¶ On leave from the Dept. of Pulmonary and Critical Care Medicine, Ajou University School of Medicine, Suwon 442-749, Korea.

‖ On leave from the Dept. of Biological Sciences, College of Natural Sciences, Chonnam National University, Gwangju 500-757, Korea.

** Present address: Dept. of Food and Nutrition, College of Home Economics, Chonnam National University, Gwangju 500-757, Korea.

‡‡ To whom correspondence should be addressed: Laboratory of Cell Signaling, NHLBI, NIH, Bldg. 50, Rm. 3523, South Dr., MSC 8015, Bethesda, MD 20892. Tel.: 301-496-9646; Fax: 301-480-0357; E-mail: sgrhee@nih.gov.

[1] The abbreviations used are: Prx, peroxiredoxin; Trx, thioredoxin; TrxR, thioredoxin reductase; DTT, dithiothreitol; CHAPS, 3-[(3-cholamidopropyl)dimethylammonio]-1-propanesulfonic acid; HPLC, high performance liquid chromatography; ESI-MS, electrospray ionization mass spectrometry; MS/MS, tandem mass spectrometry; MALDI-TOF-MS, matrix-assisted laser desorption ionization time-of-flight mass spectrometry.

(19, 24–27). The reactive cysteine is thus protected from larger oxidant molecules that contain disulfide linkages. The structures also show that the N-terminal conserved cysteine is surrounded by positively charged amino acid residues, which stabilize the thiolate ($Cys\text{-}S^-$) anion. The thiolate anion is more readily oxidized by peroxides than its protonated thiol counterpart (Cys-SH) (28). This provides the mechanistic basis for the observed sensitivity of the active-site cysteine to oxidation by peroxides.

Previously, we reported that Prx purified from yeast is readily inactivated during catalysis (1). We speculated that such inactivation occurs if the sulfenic acid moiety of the reaction intermediate is further oxidized by H_2O_2 to cysteine-sulfinic acid ($Cys\text{-}SO_2H$) before disulfide formation with Cys^{172} can occur (1). Sulfinic acid cannot be reduced by the Trx or DTT included in the assay mixture. Recently, Mitsumoto *et al.* (29) used two-dimensional PAGE to compare proteins in human umbilical vein endothelial cells before and after exposure of the cells to H_2O_2. In H_2O_2-treated cells, a number of proteins (including Prx I and Prx II) demonstrated altered migration consistent with decreased pI, suggesting that such oxidative inactivation might also occur in cells. However, these acidic Prx enzymes were not characterized in detail. We have now investigated the mechanism of human Prx I inactivation by H_2O_2. Here, we demonstrate that the enzyme inactivation and concomitant acidic shift of Prx on two-dimensional gels are due in fact to the conversion of the active-site cysteine to $Cys\text{-}SO_2H$. Furthermore, we observed that only those Prx molecules actively engaged in the catalytic cycle are vulnerable to oxidative inactivation.

MATERIALS AND METHODS

Preparation of Recombinant Proteins—The construction of a bacterial expression vector for human Prx I (pETprxI-WT) has been described (15). Two Prx I mutants in which Cys^{51} and Cys^{172} were individually replaced by serine residues (C51S and C172S, respectively) were generated by standard PCR-mediated site-directed mutagenesis with pETprxI-WT as the template and complementary primers containing a single-base mismatch that converts the codon for Cys to one for Ser. The final mutated PCR products were ligated into the pET vector to generate pETprxI-C51S and pETprxI-C172S. *Escherichia coli* BL21(DE3) competent cells (Novagen) were transformed with pETprxI-WT, pETprxI-C51S, or pETprxI-C172S; cultured at 37 °C overnight in 100 ml of LB medium supplemented with ampicillin (100 μg/ml); and then transferred to 10 liters of fresh LB medium in a Microferm fermentor (New Brunswick Scientific). When the absorbance of the culture at 600 nm reached 0.6–0.8, expression was induced by isopropyl-β-D-thiogalactopyranoside at a final concentration of 0.4 mM. After incubation for an additional 3 h, the cells were collected by centrifugation, frozen in liquid nitrogen, and stored at −70 °C until used. The recombinant proteins were purified as described (30).

Prx Assay—NADPH oxidation coupled to the reduction of H_2O_2 was monitored at 30 °C as a decrease in A_{340} using a Hewlett-Packard Model 8453 UV-visible spectrophotometer equipped with a thermostable cell holder and a multicell transport. The reaction was initiated by addition of the indicated concentration of Prx I to a 200-μl reaction mixture containing 50 mM Hepes-NaOH (pH 7.0), 1 mM EDTA, 0.8 μM TrxR, and the indicated concentrations of H_2O_2, NADPH, and Trx.

Cell Culture—HeLa S3 cells were adapted to suspension growth in Spinner minimum essential medium (Quality Biological, Inc.) supplemented with 10% (v/v) fetal bovine serum (Invitrogen). The cells were grown to a density of 1×10^6 cells/ml and maintained by dilution with fresh complete medium every 4 days.

Sample Preparation, Two-dimensional PAGE, and Immunoblot Analysis—HeLa S3 cells were rinsed three times with ice-cold phosphate-buffered saline and lysed in lysis buffer (8 M urea, 4% CHAPS, and 40 mM Tris base) by sonication in a sonic bath three to four times for 30 s. After removal of insoluble materials by centrifugation at $14{,}000 \times g$ for 30 min, cell lysates were mixed with 10 volumes of rehydration buffer (8 M urea, 2% CHAPS, 0.5% immobilized pH gradient buffer, 20 mM DTT, and 0.005% bromphenol blue) and loaded onto immobilized pH gradient strips (pH 3–10, nonlinear). Isoelectric focusing on an IPGPhor isoelectrofocusing unit (Amersham Biosciences) and preparation (reduction and alkylation) of the immobilized pH gradient strips for the second-dimension SDS-PAGE were carried out according to the procedures recommended by the manufacturer. SDS-PAGE was conducted on 12% gels using an Amersham Biosciences SE600 vertical unit, and the protein spots were visualized by staining with silver nitrate. For immunoblot analyses of Prx enzymes, proteins on two-dimensional gels were transferred electrophoretically to a nitrocellulose membrane, and the membrane was incubated with rabbit antibodies to Prx I. Immune complexes were detected with horseradish peroxidase-conjugated secondary antibodies and enhanced chemiluminescence reagents (Amersham Biosciences or Pierce). Silver-stained two-dimensional gels were scanned with a Molecular Dynamics SI personal densitometer.

Reverse-phase High Performance Liquid Chromatography (HPLC)—Reverse-phase HPLC analyses were performed using an Agilent 1100 HPLC system with a Vydac 218TP54 column (0.47 mm × 25 cm). For protein analysis, injected samples were eluted at 1 ml/min with a 5–35% (v/v) acetonitrile/water gradient containing 0.04% (v/v) trifluoroacetic acid over 15 min and with a 35–60% gradient over the next 15 min. Gradients of 5–10% over 10 min, 10–40% over 30 min, and 40–60% over 30 min were used for peptide analysis.

Electrospray Ionization Mass Spectrometry (ESI-MS) Analysis of Prx I Proteins and Sequence Analysis of Tryptic Peptides—A Finnigan MAT LCQ electrospray ion-trap mass spectrometer was used for analysis of Prx I proteins and sequence analysis of Cys^{51}-containing peptides. Dried HPLC fractions dissolved in 75% acetonitrile and 0.1% acetic acid were introduced at 1 μl/min using a syringe pump. Data were collected for positive ions at 300–2000 *m/z* using the following settings: capillary temperature, 215 °C; maximum ion inject time, 100 ms; full scan target, 9×10^7; and three microscans/full scan. For proteins, ESI-MS spectra were obtained and used to calculate the masses of proteins by deconvolution using Finnigan MAT BioWorks software. For sequence analysis of peptides, once the parent ions were identified, the mass spectrometer was set up to obtain collision-induced dissociation MS/MS spectra of the parent ions. The instrument for MS/MS spectra was configured as follows: capillary temperature, 215 °C; maximum ion inject time, 100 ms; full scan target, 2×10^7; three microscans/full scan; mass window, 2.5; and collision energy, used within a range of 0–50%.

MALDI-TOF-MS—Mass spectrometry analysis of the tryptic peptides was performed on a Voyager-STR MALDI-TOF instrument (PerSeptive Biosystems, Framingham, MA) equipped with a nitrogen laser. Samples were dissolved in 50% acetonitrile and 5% formic acid, mixed with 10 mg/ml 3,5-dimethoxy-4-hydroxycinnamic acid (sinapinic acid; Aldrich) in 0.1% trifluoroacetic acid and 70% acetonitrile, and spotted on a sample plate. The spectra were obtained in the positive-ion reflector or linear mode with delayed extraction under standard conditions. Spectra were analyzed using DataExplorer software (PerSeptive Biosystems). Standard peptides were used for calibration of peptides, whereas apomyoglobin and carbonic anhydrase were used as internal standards for mass scale calibration of proteins.

RESULTS

Prx I Inactivation in Vitro—The peroxidase activity of human Prx I was monitored by following the decrease in A_{340} attributable to the oxidation of NADPH in a reaction mixture containing NADPH, Trx, TrxR, and varying concentrations of H_2O_2. The initial rate of NADPH oxidation (the slope at $t = 0$) was independent of H_2O_2 at saturating concentrations (0.1–1 mM) (K_m for $H_2O_2 < 20$ μM (31)) (Fig. 1*A*). However, the rate decreased with time, and the higher the H_2O_2 concentration, the faster the rate of decrease. The H_2O_2 concentration dependence of this decrease is shown more quantitatively by plotting the rate of NADPH oxidation (the first derivative of the NADPH oxidation curve) *versus* time (Fig. 1*B*). Replenishment of Prx I was shown to restore the enzyme rate, indicating that the markedly decreased NADPH oxidation rate was not attributable to exhaustion of substrate or to product inhibition (data not shown). Reactions containing 200 μM H_2O_2 were stopped at 0, 60, and 150 s, and the resulting samples were subjected to two-dimensional PAGE analysis. A single spot at a position corresponding to a pI value of 8.1 (the theoretical pI of Prx I is 8.2) was observed at 0 s. At 60 s, however, a new spot whose intensity was similar to that of the original spot appeared at a more acidic position (pI 7.6). At 150 s, the intensity of the acidic

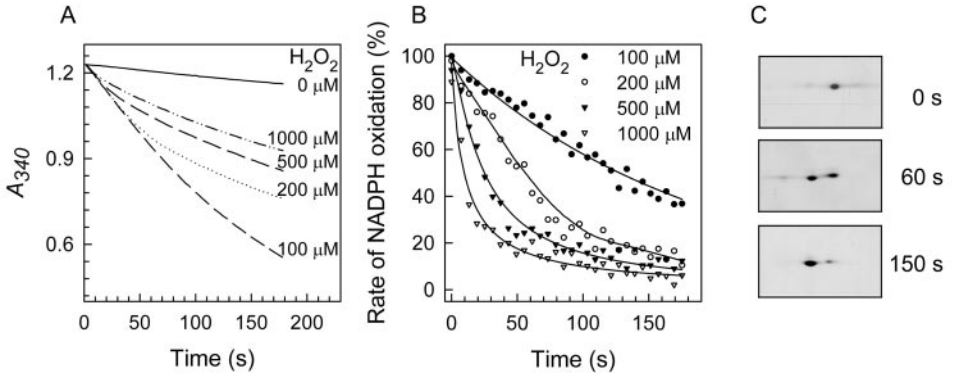

FIG. 1. **Inactivation of Prx I peroxidase activity.** *A*, NADPH oxidation coupled by TrxR, Trx, and Prx I to the reduction of H_2O_2 was monitored at 30 °C as a decrease A_{340} in a 200-μl peroxidase assay mixture containing 50 mM Hepes-NaOH (pH 7.0), 1 mM EDTA, 200 μM NADPH, 80 nM TrxR, 2.5 μM Trx, 2.4 μM Prx I, and the indicated amounts of H_2O_2. *B*, the rate of NADPH oxidation at each time point reflected by the first derivative of the curves in *A* was expressed as a percentage of the initial enzyme rate (the first derivative at $t = 0$). *C*, an aliquot (10 μl) of the 200 μM H_2O_2-containing reaction mixture was taken at 0, 60, and 150 s and subjected to two-dimensional PAGE. Only the regions of the silver-stained gels containing Prx I spots are shown.

spot was enhanced at the expense of the original spot. The increasing proportion of the acidic species compared with the original spot is consistent with the notion that the 50 and 80% decreases in rate observed at 60 and 150 s, respectively, are related to the conversion of Prx I to a more acidic derivative.

Selective Hyperoxidation of Cys^{51}-SH to Cys^{51}-SO_2H by H_2O_2—To identify the modification responsible for the acidic shift, Prx I was oxidized for 5 min in the presence of 1 mM H_2O_2 and 10 mM DTT. Reduced and oxidized enzymes were separated from the reaction mixture by reverse-phase HPLC (Fig. 2*A*). The molecular masses of the separated proteins were measured by ESI-MS (Fig. 2*B*). The masses calculated from *m/z* and total charge of multiply charged ions of the reduced and oxidized enzymes were 21,979 and 22,011 Da, respectively. The mass of the reduced enzyme was in good agreement with the theoretical mass of 21,979.2 Da. The difference of 32 mass units between the reduced and oxidized Prx I enzymes suggests the presence of two additional oxygen atoms in the oxidized species.

To determine the site of oxidation, the reduced and oxidized Prx I enzymes separated in Fig. 2*A* were digested with trypsin, and the resultant peptides were fractionated by reverse-phase HPLC (Fig. 2*C*). The HPLC elution profiles of the reduced and oxidized Prx I peptides were nearly identical except between 48 and 56 min (Fig. 2*C*). Major peptide peaks from the reduced and oxidized proteins were collected and analyzed by MALDI-TOF-MS, enabling the assignment of 12 such peaks to defined fragments of Prx I. In addition to the disulfide-forming Cys^{51} and Cys^{172} residues, Prx I contains two additional cysteine residues at positions 70 and 82. In both the reduced and oxidized states, the Cys^{172}-containing peptide encompassing residues 168–189 eluted from the HPLC column at 26.1 min. Peptides containing both Cys^{70} and Cys^{82} were also unchanged: in both states, the peptides encompassing residues 67–91 (representing one missed trypsin cleavage site at Lys^{67}) and residues 68–91 eluted at 35.5 and 36.8 min, respectively. However, retention of Cys^{51}-containing peptides was altered by oxidation. In the reduced state, the peptides encompassing residues 27–61 (representing two missed trypsin cleavage sites at Lys^{34} and Lys^{36}), residues 35–61 (representing one missed cleavage site at Lys^{36}), and residues 37–61 eluted at 50.8, 51.7, and 55.1 min, respectively (Fig. 2*D*). In the oxidized protein, however, none of these peaks corresponding to the three Cys^{51}-containing peptides were observed. Instead, several peaks eluted near the expected positions. When the peaks at 49.7, 50.4, and 53.0 min were analyzed by MALDI-TOF-MS, each of them displayed a dominant and a minor ion separated by 16 mass units (Fig. 2*D*). Furthermore, the dominant ions derived from the oxidized peptides eluting at 49.7, 50.4, and 53.0 min were each larger by 32 mass units than those derived from reduced peptides encompassing residues 27–61, 35–61, and 37–61, respectively (Fig. 2*D* and Table I). These results support a model wherein Cys^{51}-SH, but not Cys^{70}-SH, Cys^{82}-SH, or Cys^{172}-SH, is hyperoxidized by H_2O_2 to Cys-SO_2H and cysteic acid (Cys-SO_3H).

To demonstrate directly the formation of Cys^{51}-SO_2H, the amino acid sequence of the dominant ion ($[M + 2H]^{2+}$, *m/z* 1535.90) derived from peptide 37–61 was determined from the masses of the fragments arising from collision-induced dissociation of the peptide. The collision-induced dissociation MS/MS spectrum of the ion is shown in Fig. 2*E*, along with the interpretation. The major daughter ions are y_{10} (*m/z* 1148.5) and b_{15} (*m/z* 1922.5) ions, which derive from cleavage of the peptide bond between Cys^{51} and Pro^{52}. The mass differences between b_{14} and b_{15} (135.2 Da), between y_{10} and y_{11} (135.0 Da), and between z_{10} and z_{11} (135.0 Da) clearly indicate the presence of Cys-SO_2H at Cys^{51}.

Mass spectral analysis of the tryptic peptides suggested that peroxide oxidation of Prx I Cys^{51} yielded mainly Cys^{51}-SO_2H, but also Cys^{51}-SO_3H to a lesser extent. In Fig. 2, Prx I was digested with trypsin for only 3 h before HPLC analysis. However, when oxidized Prx I was digested overnight with trypsin, Cys^{51}-SO_3H-containing peptides became the major products (data not shown). Furthermore, purified Cys^{51}-SO_2H-containing peptides were slowly autoxidized to Cys^{51}-SO_3H-containing peptides upon exposure to air (data not shown). However, longer exposure of intact Prx I to either H_2O_2 or air did not increase cysteic acid content (data not shown). Therefore, it appears that the formation of cysteic acid derivatives is the result of the air oxidation of Cys-SO_2H-containing peptides. The sensitivity of Cys-SO_2H to air has been reported (32).

Effect of Mutation of Cys^{51} and Cys^{172} on the Hyperoxidation of Prx I—Cysteines 51 and 172 were individually replaced by serine residues to generate the C51S and C172S mutant enzymes, respectively. The wild-type and mutant enzymes were subjected to two-dimensional PAGE analysis before and after incubation with a peroxidase reaction mixture containing H_2O_2, NADPH, Trx, and TrxR (Fig. 3). As observed in Fig. 1*C*, the wild-type enzyme migrated predominantly to the more acidic position upon incubation with H_2O_2, suggesting that Cys^{51}-SH was hyperoxidized to Cys-SO_2H. As expected, no such shift was observed for C51S. C172S, which is catalytically inactive because Cys^{172}-SH is required for disulfide formation by Cys^{51}-SOH, did not undergo hyperoxidation. In contrast, when reducing equivalents were provided by DTT rather than

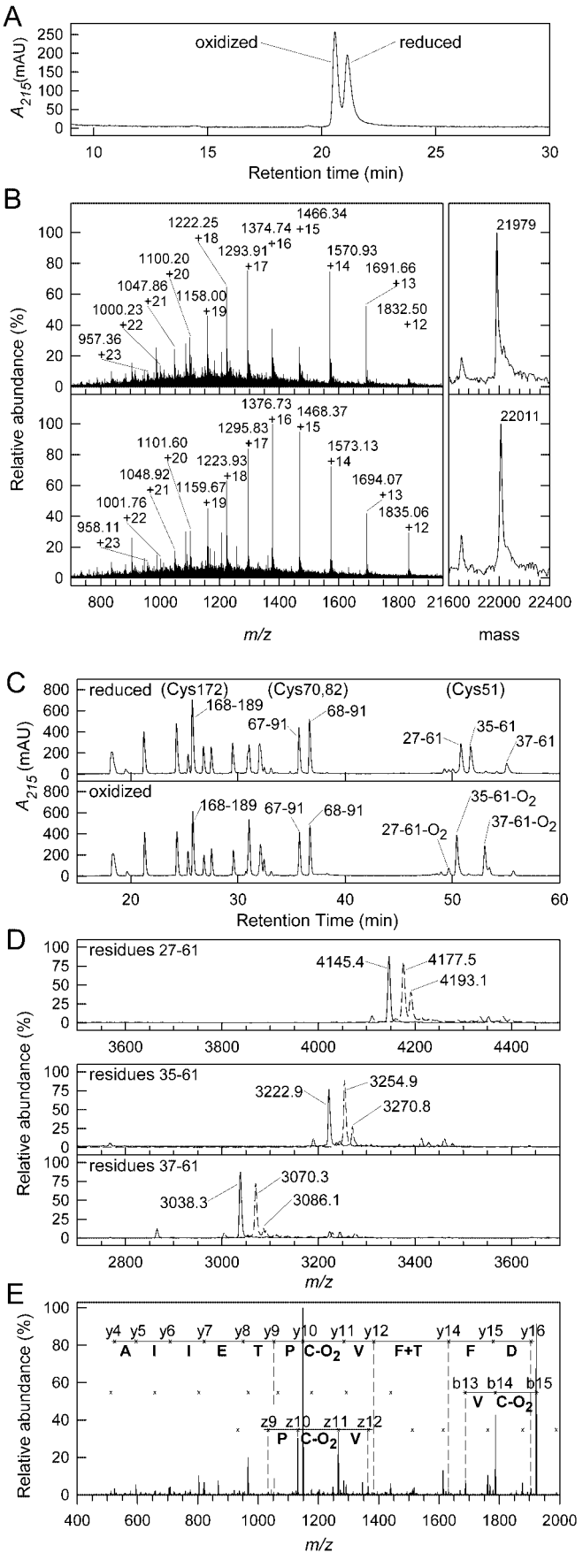

FIG. 2. **Mass spectrometry analysis of reduced and oxidized Prx I proteins.** *A*, Prx I (200 μg) was incubated for 5 min at 30 °C in a 1-ml reaction mixture containing 50 mM Hepes-NaOH (pH 7.0), 1 mM H_2O_2, 1 mM EDTA, and 10 mM DTT. After bringing the solution to pH 2 by trifluoroacetic acid, the reaction mixture was subjected to reverse-phase HPLC to fractionate the reduced and oxidized enzymes, with elution monitored on the basis of A_{215}. *B*, shown are the results from ESI-MS analysis of reduced Prx I (*upper panels*) and oxidized Prx I (*lower panels*). The spectra of multiply charged ions with *m/z* values and corresponding total charges (*left panels*) and deconvoluted spectra derived from these component ions with calculated masses (*right panels*) are shown. The calculated masses of reduced Prx I (21,979 Da) and oxidized Prx I (22,011 Da) differ by 32 Da. *C*, reduced and oxidized Prx I proteins (100 μg each) were separately digested with 1 μg of bovine trypsin at 37 °C for 3 h, and the resulting peptides were fractionated by HPLC on a C_{18} column, with elution monitored on the basis of A_{215}. The relevant cysteine residues, as well as the start-to-end amino acid residues within the Prx sequence, are indicated above the peaks for Cys-containing peptides. *mAU*, milli-absorbance units. *D*, the three Cys^{51}-containing peptides encompassing residues 27–61 (*upper panel*), residues 35–61 (*middle panel*), and residues 37–61 (*lower panel*) were collected and subjected to MALDI-TOF-MS analysis. The spectra of the corresponding peptides from reduced (*solid lines*) and oxidized (*dashed lines*) enzymes were superimposed to highlight their mass differences. Average *m/z* values are indicated for major peaks. *E*, shown is the collision-induced dissociation MS/MS spectrum of $[M + 2H]^{2+}$ ions of the peptide containing residues 37–61 (*m/z* 1535.90) derived from the oxidized enzyme. Peaks corresponding to b, y, and z daughter ions are indicated (×), and selected ions neighboring Cys^{51} are labeled with the sequence of the peptide. *C-O*$_2$ denotes Cys-SO_2H.

by the Trx system (Trx, TrxR, and NADPH), C172S became hyperoxidized just as the wild-type enzyme did, whereas C51S was still resistant to hyperoxidation. As previously shown with a yeast Prx mutant in which the C-terminal conserved Cys was changed to Ser (1), C172S is fully active when supported by DTT even though it lacks peroxidase activity in the presence of the Trx system (data not shown). Such catalysis is possible because a small diffusible thiol molecule like DTT can replace Cys^{172}-SH in the formation of a disulfide with Cys^{51}-SOH. The disulfide is subsequently reduced by DTT. These results indicate that oxidation of Cys^{51}-SH to Cys^{51}-SO_2H occurs only when Prx is engaged in the catalytic cycle.

Effect of Trx Concentration on the Hyperoxidation of Prx I—To further examine whether the accumulation of the hyperoxidized protein requires continuous passage through the catalytic cycle, Prx I was inactivated by incubation with H_2O_2, NADPH, TrxR, and varying concentrations of Trx. An aliquot of the reaction mixture was removed at various times and assayed for peroxidase activity by measuring NADPH oxidation coupled to H_2O_2 reduction. For each Trx concentration, the initial rate of NADPH oxidation was plotted against duration of inactivation to yield rates of enzyme inactivation (Fig. 4*A*). Prx I inactivation proceeded slowly in the absence of Trx and increased gradually with increasing Trx concentrations, reaching saturation at 4 μM Trx. The Trx dependence of inactivation is displayed by plotting the residual activities measured after a 3-min incubation with the inactivation reaction mixture against Trx concentration. Half-maximal inactivation occurred at <0.5 μM Trx. When either TrxR or NADPH was omitted from the inactivation mixture, inactivation essentially ceased, as observed in the absence of Trx (data not shown). These results suggest that active catalysis renders Prx I molecules susceptible to peroxidation.

Prx I Inactivation at Steady-state Concentrations of H_2O_2—In the experiments described above, relatively high nonphysiological concentrations of H_2O_2 (0.1–1 mM) were employed to inactivate Prx I. These conditions were required because H_2O_2 is continuously consumed by Prx in the presence of the Trx system. Moreover, in practice, quantitative monitoring of Prx I-coupled NADPH consumption requires H_2O_2 concentrations higher than 0.1 mM. No reliable method to measure the intracellular concentration of H_2O_2 is currently available. However, it is predicted that H_2O_2 levels in normal cells are

TABLE I
Characterization of Cys^{51}-containing peptides

Residues	Retention time	Mass		Sequence
		Theoretical[a] *m/z*	Observed[b] *m/z*	
	min			
27–61[c]	50.8	4145.8	4145.4	DISLSDYKGKYVVFFFYPLDFTFVCPTEIIAFSDR
27–61-O_2 [d]	49.7	4177.8	4177.5	
27–61-O_3 [e]		4193.8	4193.1	
35–61[c]	51.7	3223.8	3222.9	GKYVVFFFYPLDFTFVCPTEIIAFSDR
35–61-O_2 [d]	50.4	3255.8	3254.9	
35–61-O_3 [e]		3271.8	3270.8	
37–61[c]	55.1	3038.5	3038.3	YVVFFFYPLDFTFVCPTEIIAFSDR
37–61-O_2 [d]	53.0	3070.5	3070.3	
37–61-O_3 [e]		3086.5	3086.1	

[a] Theoretical average *m/z* values of singly charged ions ($[M + H]^+$) calculated using GPMAW software (Lighthouse Data, Odense, Denmark).
[b] Average of at least three separate experiments with S.D. <0.02%.
[c] Cys^{51}-SH-containing peptide.
[d] Cys^{51}-SO_2H-containing peptide.
[e] Cys^{51}-SO_3H-containing peptide.

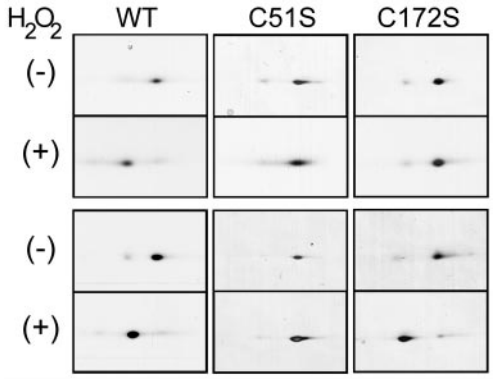

FIG. 3. **Effects of the mutation of Cys^{51} and Cys^{172} on the hyperoxidation of Prx I.** Wild-type (*WT*) Prx I and the indicated mutants (8 μg each) were incubated for 3 min at 30 °C in a 100-μl reaction mixture containing 50 mM Hepes-NaOH (pH 7.0), 1 mM EDTA, 1 mM H_2O_2, and either the Trx system (1 mM NADPH, 80 nM TrxR, and 2.5 μM Trx) (*upper panels*) or 10 mM DTT (*lower panels*). An aliquot (10 μl) of the reaction mixture was subjected to two-dimensional PAGE, and the proteins were visualized by silver staining.

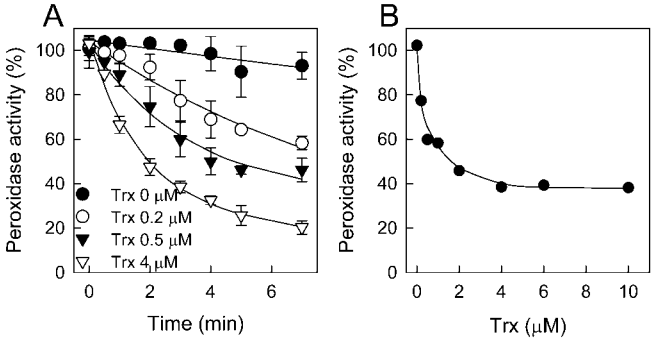

FIG. 4. **Effect of Trx concentration on the hyperoxidation of Prx I.** *A*, Prx I (50 μg) was incubated at 30 °C in a 150-μl inactivation mixture containing 50 mM Hepes-NaOH (pH 7.0), 1 mM EDTA, 1 mM NADPH, 160 nM TrxR, 1 mM H_2O_2, and the indicated concentrations of Trx. At the indicated times, 20 μl of the inactivation mixture was added to a 200-μl peroxidase assay mixture containing 50 mM Hepes-NaOH (pH 7.0), 1 mM EDTA, 200 μM NADPH, 80 nM TrxR, 10 μM Trx, and 100 μM H_2O_2; and peroxidase activity was derived from A_{340} measurements made in a Hewlett-Packard multichannel UV-visible spectrophotometer. The residual peroxidase activity measured at various times after exposure to the inactivation mixture is expressed as a percentage of the peroxidase activity at 0 min of exposure. *B*, the residual peroxidase activity at 3 min from *A* is plotted against the concentration of Trx.

maintained at very low concentration by various antioxidant enzymes and small molecules that counteract H_2O_2 production. To mimic physiological conditions, H_2O_2 was produced with the use of glucose and glucose oxidase. Prx I-dependent NADPH oxidation was monitored in the presence of different concentrations of glucose oxidase without varying the other reaction components (Prx I, Trx, TrxR, NADPH, and glucose). The levels of H_2O_2 produced by the glucose oxidase concentrations used in these experiments did not exceed the H_2O_2 elimination capacity of Prx I as long as sufficient NADPH remained.

In the presence of 45 milliunits of glucose oxidase, Prx I inactivation, reflected by the rate of NADPH oxidation (first derivative of the NADPH oxidation curve), occurred gradually during the first 1100 s, at which point NADPH was nearly depleted (Fig. 5*A*). The H_2O_2 concentration remained below the limit of detection (<1 μM) until NADPH depletion and increased rapidly thereafter. Both the rate of Prx I catalysis (NADPH consumption) and the rate of Prx I inactivation prior to NADPH depletion increased in a glucose oxidase-dependent manner when the amount of glucose oxidase was increased to 60 and 80 milliunits (Fig. 5, *B* and *C*). However, the concentration of H_2O_2 remained below the sensitivity limit of analysis until just before the point of NADPH depletion, as with reaction conditions obtained with 45 milliunits of glucose oxidase. The NADPH oxidation rate (v) was fit to an equation describing the rate of the inactivation reaction as $v = v_0^{-k_i t}$ to yield an initial rate (v_0) and inactivation rate constant (k_i) (Table II). The peroxidase catalytic rate constant k_{cat} in Table II was calculated from the equation $v_0 = k_{cat}[E]_0$, where $[E]_0$ is the initial concentration of Prx I (0.4 nmol). The k_i/k_{cat} ratio represents the fraction of Prx I molecules that are inactivated per catalytic turnover. The k_i/k_{cat} ratios derived from reactions employing 45, 60, and 80 milliunits of glucose oxidase were similar (Table II). The average k_i/k_{cat} was 7.2×10^{-4}, indicating that 0.072% of Prx I molecules undergo inactivation per turnover when H_2O_2 is maintained at a steady-state level. When 100 milliunits of glucose oxidase were added, the concentration of H_2O_2 steadily increased, and the rate of inactivation also increased steadily before the rapid phase of inactivation (Fig. 5*D*). Therefore, these data were not used to calculate kinetic parameters.

Prx Oxidation in Cells Exposed to H_2O_2—We examined whether Prx I molecules become hyperoxidized in cells exposed to H_2O_2. When HeLa cells were incubated for 30 min with various concentrations of H_2O_2, the dose-dependent conversion of Prx I to a more acidic spot was apparent (Fig. 6*A*). Mixing experiments showed that the acidic Prx I protein from H_2O_2-treated cells comigrated precisely with Prx I oxidized *in vitro* (Fig. 6*B*). Small quantities of the acidic Prx I form were con-

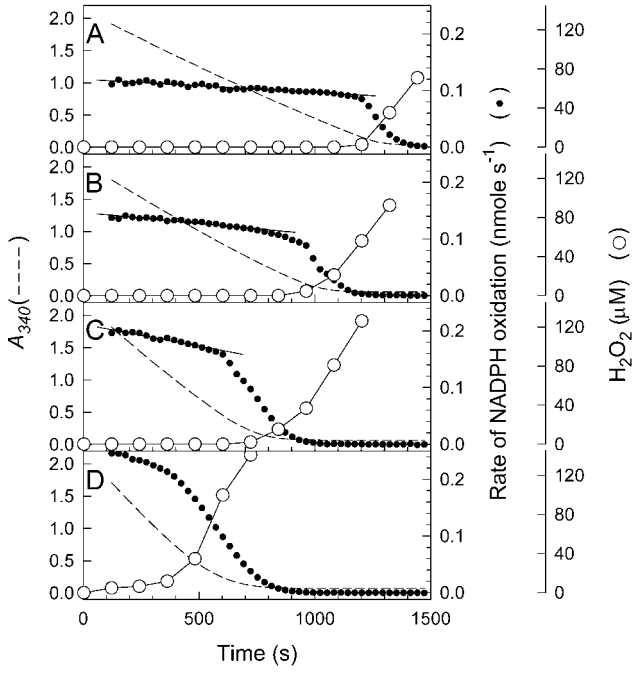

FIG. 5. **Inactivation of Prx I at steady-state concentrations of H_2O_2.** The peroxidase activity of Prx I was monitored at 30 °C as a decrease in A_{340} (*dashed lines*) in a cuvette (1.0-cm path length) containing 50 mM Hepes-NaOH (pH 7.4), 0.35 mM NADPH, 47.5 nM TrxR, 5.2 μM Trx, 1 μM Prx I, and 2.5 mM glucose in a total volume of 400 μl. The reaction mixtures were saturated with oxygen before the Prx I-coupled NADPH oxidation reactions were started by addition of 45 milliunits (*A*), 60 milliunits (*B*), 80 milliunits (*C*), and 100 milliunits (*D*) of glucose oxidase. The rate of NADPH oxidation (nmol s^{-1}; ●) at each time point was derived from the first derivative of each NADPH oxidation curve using Chemstation software (Agilent, Palo alto, CA) installed in a Hewlett-Packard Model 8453 UV-visible spectrophotometer. The rate values (v) up to 1100 s (*A*), 750 s (*B*), and 480 s (*C*) were fit to the equation $v = v_0^{-k_i t}$ to yield the indicated lines (*solid lines*), from which the initial rates (v_0) and inactivation rate constants (k_i) listed in Table II were derived. Data obtained during the first 100 s were not included because of the disturbance following addition of glucose oxidase and the possibility that the level of H_2O_2 had not reached a steady state. The concentration of H_2O_2 (○) was monitored during the NADPH oxidation reaction according to the procedure of Gay and Gebicki (44). The reaction mixture (18 μl) was removed at the indicated times and added to a 200-μl peroxide assay mixture containing 0.25 mM ferrous ammonium sulfate, 0.25 mM xylenol orange, and 110 mM perchloric acid. After a 30-min incubation at room temperature, A_{560} of the ferric xylenol complex was measured against a blank, which contained all the components except glucose oxidase. H_2O_2 concentrations were estimated from a standard curve generated with known concentrations of H_2O_2.

TABLE II
Kinetic parameters for Prx I inactivation at steady-state levels of H_2O_2

GO[a]	v_0 [b]	k_i [b] × 10^4	k_{cat} [c]	k_i/k_{cat} × 10^4
milliunits	*nmol s^{-1}*	*s^{-1}*	*s^{-1}*	
45	0.12	2.2	0.30	7.3
60	0.15	2.6	0.37	7.1
80	0.22	3.7	0.53	7.1

[a] Glucose oxidase.
[b] v_0 (initial rate of NADPH oxidation) and k_i (inactivation rate constant) obtained as described for Fig. 5.
[c] Calculated according to the following equation: $v_0 = k_{cat}[E]_0$, where $[E]_0$ = 40 nmol.

sistently observed in cells that had not been exposed to H_2O_2, suggesting that hyperoxidation also occurs in cells grown under normal conditions. To characterize the Cys oxidation state of Prx I in H_2O_2-treated cells, oxidized Prx I was purified from HeLa cells that had been exposed to 200 μM H_2O_2 for 30 min by subjecting the cell extracts to sequential HPLC on TSK DEAE-5PW, TSK heparin-5PW, and Vydac C_{18} columns (data not shown). Reduced Prx I was also purified similarly from HeLa cells not exposed to H_2O_2. ESI-MS analysis revealed the difference of 32 mass units between the reduced and oxidized Prx I forms, suggesting that one of the Prx I Cys residues is in the sulfinic acid state in H_2O_2-treated cells (data not shown).

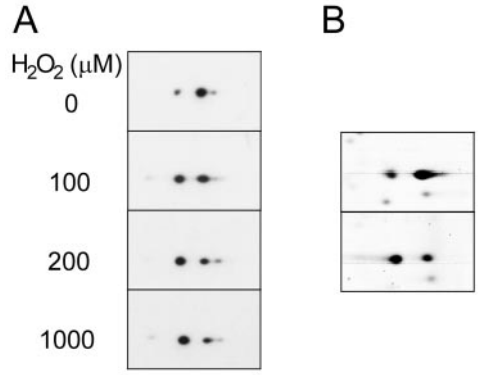

FIG. 6. **Prx oxidation in HeLa cells exposed to H_2O_2.** *A*, HeLa cells were incubated for 30 min with the indicated concentrations of H_2O_2. Cell lysates (20 μg) were then analyzed by two-dimensional PAGE, and the resulting gels were subjected to immunoblot analyses with antibodies to Prx I. *B*, lysates of HeLa cells treated with 100 μM H_2O_2 were mixed with reduced (*upper panel*) or oxidized (*lower panel*) recombinant Prx I, and the mixtures were analyzed by two-dimensional PAGE. Only the regions of the silver-stained gels containing Prx I spots are shown.

DISCUSSION

The catalytic cycle using Prx I as the archetype member of 2-Cys Prx enzymes is outlined in Fig. 7*A*. This model was initially proposed on the basis of studies with yeast Prx (1, 14) and later substantiated by observations made with other 2-Cys Prx enzymes, including mammalian Prx V (13), bacterial AhpC (33), and trypanosomal TXNPx (34). During catalysis, Cys^{51}-SH is selectively oxidized because this N-terminal conserved cysteine exists as a thiolate anion, whereas the other cysteines remain protonated at neutral pH. Cys^{51}-SOH resulting from quantitative oxidation by H_2O_2 then reacts with the C-terminal conserved Cys^{172}-SH of the other subunit to form a disulfide. This intersubunit disulfide is reduced by Trx to complete one cycle of catalysis.

Sulfenic acids are usually very unstable and highly reactive; they readily react with any accessible thiol to form a disulfide or are prone to further oxidation to sulfinic acids or sulfonic acids (35–37). Nevertheless, stable intermediates containing Cys-SOH have been identified in various enzymes, including bacterial NADH peroxidase (32, 38, 39) and mammalian 1-Cys Prx (Prx VI) (19) using chemical methods, NMR, and x-ray crystallography. The major factor underlying the stability of the sulfenic acid intermediate in these proteins is the absence of a proximal partner Cys-SH. Stability is also attributable to the inaccessibility of Cys-SOH and participation of the sulfenate ion (Cys-SO^-) in charge or hydrogen-bonding interactions with other residues. For example, the x-ray structure of oxidized mammalian Prx VI revealed that Cys^{47}-SO^- not only has no neighboring Cys-SH, but also is stabilized in a deep narrow pocket through interactions with two positively charged residues (Arg^{132} and His^{39}) and hydrogen bonding with a water molecule (19). Arg^{132} and His^{39} are likely the same residues that promote ionization of Cys^{47}-SH in the reduced enzyme. In particular, Arg^{132} of Prx VI, which is equivalent to Arg^{127} of Prx I, is conserved in Prx enzymes from all species (2, 3).

Our data presented here reveal that the Cys^{51}-SOH intermediate of Prx I is occasionally oxidized to Cys-SO_2H. Unlike disulfide and sulfenic acid intermediates, Cys-SO_2H cannot be

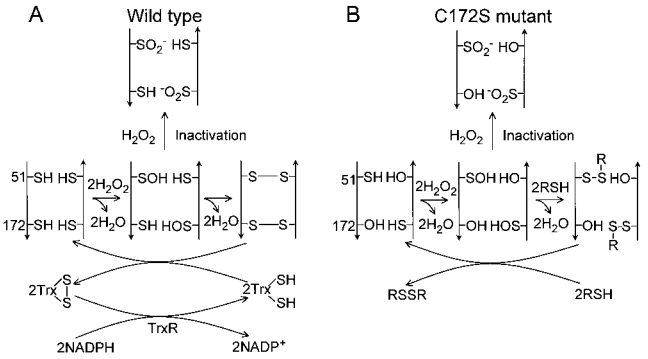

FIG. 7. **Catalytic cycles of the wild-type (*A*) and C172S mutant (*B*) Prx I enzymes and their inactivation mechanisms.** *Straight arrows* in Prx I molecules indicate C termini.

reduced by Trx or DTT. Consequently, hyperoxidation leads to accumulation of inactivated enzyme, which is responsible for the gradual decay of Prx-dependent NADPH oxidation shown in Figs. 1, 4, and 5. The rate of enzyme inactivation increased when H_2O_2 concentration was increased in the range of 0.1–1 mM (Fig. 1), despite an observed K_m for H_2O_2 of <20 μM (a definite K_m value could not be determined because the changes in A_{340} were not large enough to allow evaluation of initial rates) (31). These observations indicate that although the initial oxidation of Cys^{51}-SH is achieved by H_2O_2 attracted to the active-site pocket with an affinity constant of <20 μM, subsequent oxidation to Cys-SO_2H depends upon collision with unbound or more weakly associated H_2O_2 molecules. Nonetheless, as shown in Fig. 4, incubation with 1 mM H_2O_2 alone did not cause significant inactivation. Prx I inactivation appeared to occur exclusively during active passage through the catalytic cycle, and increased catalytic rates were associated with increased rates of inactivation. One possible explanation for the dependence of inactivation on catalytic rate is that Cys^{51} is susceptible to hyperoxidation only in the sulfenic acid state. Once Cys^{51}-SH has established a disulfide with Cys^{172}, this disulfide is no longer vulnerable to oxidation. Therefore, when enzyme molecules are found in the disulfide state with higher frequency because of a limited supply of reducing equivalents (Trx), the likelihood of hyperoxidation diminishes.

However, immunity of disulfide linkages to H_2O_2 cannot account for the observation that hyperoxidation of the C172S mutant occurred in the presence of H_2O_2 plus DTT, but not in the presence of H_2O_2 alone (Fig. 3). Cys^{51}-SH of the mutant protein was converted to the sulfenic acid state by H_2O_2, as evidenced by the fact that the C172S enzyme demonstrated peroxidase activity in the presence of DTT. C172S could function as a peroxidase in the presence DTT or 2-mercaptoethanol because these small molecules can donate thiol groups to disulfide linkages with Cys^{51}-SOH and also reduce the resultant disulfides (Fig. 7*B*). Thus, C172S is similar to Prx VI, which contains only one conserved cysteine in the N-terminal domain and is catalytically active in the presence of DTT, but not Trx (18). The sulfenic acid oxidation state of the N-terminal conserved cysteine within oxidized Prx VI was demonstrated by x-ray structural analysis (19) and in an oxidized AhpC mutant in which the C-terminal Cys residue was replaced by Ser using a chemical method (33). The resistance of Cys^{51}-SOH to further oxidation in the presence of H_2O_2 alone suggests that the sulfenyl moiety is either shielded from H_2O_2 or stabilized by surrounding residues such that its exposure to further oxidation is diminished. Perhaps nucleophilic attack of the sulfur atom of Cys^{51}-SOH by either Cys^{172} or DTT promotes structural shifts that expose and/or destabilize the sulfenyl moiety, rendering it reactive with H_2O_2. This would be consistent with the observed catalysis-dependent susceptibility of Cys^{51}-SOH in both the wild-type and C172S mutant enzymes. A model invoking major structural changes finds strong support in the known three-dimensional structures of Prx enzymes.

The three-dimensional structures of four 2-Cys Prx enzymes (Prx I, Prx II, TXNPx, and AhpC) and one 1-Cys Prx enzyme (Prx VI) have been determined (19, 24–27). Direct structural comparisons of the same Prx enzyme differing only in oxidation state at the N-terminal conserved cysteine are not available. However, examination of the structures reveals that in reduced enzymes, the sulfur atoms of the N- and C-terminal conserved cysteine residues are too far apart to react with each other (3, 25, 26). Thus, disulfide formation requires significant conformational changes that include unwinding of the active-site N-terminal helix and the movement of four loops (3, 25–27). Particularly valuable information was provided by the x-ray structure of Prx II that was purified from aged erythrocytes, in which Cys^{51} is found in the sulfinic acid state (25). The sulfinic acid moiety is buried within the active-site pocket, whereas the thiol of Cys^{172} is partially exposed, and the sulfur-oxyacid makes a salt bridge with Arg^{127}, the same residue that interacts with the thiolate anion of Cys^{51} in reduced form. As in the reduced enzyme, Cys^{51}-SO_2^- and Cys^{172}-SH are found far apart, with their sulfur atoms separated by ~13 Å (25). Other structural features also indicate that the sulfinic enzyme closely resembles its reduced form (25). On the basis of this information, we can predict that the sulfenic acid moiety of Prx I Cys^{51}, also a sulfur-oxyacid group, is likewise shielded from solvent and stabilized by forming a salt bridge with Arg^{127} such that it is impervious to further oxidation to sulfinic acid. To accommodate disulfide formation between Cys^{51}-SOH and either Cys^{172} or DTT, parts of the Prx protein must undergo major rearrangements (40). These conformational changes that necessarily accompany the catalytic cycle are likely to deprive the sulfenic acid moiety of shielding and stabilization, increasing its susceptibility to further oxidation.

Hyperoxidation to the sulfinic acid state is not a process that occurred only in the presence of high nonphysiological levels of H_2O_2. This hyperoxidation also took place, albeit slowly, when H_2O_2 levels were maintained at low steady-state concentrations (<1 μM) using glucose and glucose oxidase (Fig. 5). The limited sensitivity of the available analytic methods precluded measurement of H_2O_2 concentration in the peroxidase reaction. Nevertheless, H_2O_2 concentrations were expected to be constant over the time course of the reaction, independent of glucose oxidase concentration, as long as elimination by Prx I was faster than production by glucose oxidase. Under such steady-state conditions, the rate of Prx I inactivation increased as the rate of H_2O_2 production by glucose oxidase (*i.e.* the rate of H_2O_2 elimination by Prx I) increased. This is consistent with the notion that Prx I molecules are inactivated while engaged in the catalytic cycle and that the likelihood of inactivation increases as the enzyme rate increases. On the basis of data obtained at three different glucose oxidase concentrations, we estimated that 0.072% of Prx I molecules become hyperoxidized during each round of catalysis.

Our two-dimensional PAGE analysis showed a small spot of hyperoxidized Prx I from lysates derived from cells grown in the absence of H_2O_2 (Fig. 6), indicating that the hyperoxidation of Prx I takes place in cells cultured under normal conditions. Hyperoxidation increased rapidly when increasing amounts of H_2O_2 were applied to the cultures. While our studies were underway, Rabilloud *et al.* (41) reported that treatment of several different cells with alkyl hydroperoxide causes an acidic shift of Prx II and Prx III on two-dimensional gels. From the results of in-gel tryptic digestion followed by mass spectral

analysis, they concluded that the shift is attributable to the oxidation of the N-terminal conserved cysteine to a sulfonic acid derivative. However, our results suggest that the acidic shift is associated with the formation of a sulfinic acid derivative, not a sulfonic acid derivative. We found that the sulfinic acid oxidation state in the intact enzyme is stable, probably because the sulfinic acid group is stabilized through a salt bridge to Arg^{127}. When the sulfinic Prx protein was digested with trypsin, the sulfinic acid group was slowly autoxidized to the sulfonic acid state, suggesting that the sulfonic acid state reported by Rabilloud *et al.* (41) might be due to a stronger oxidation potential of alkyl hydroperoxide or an artifact of air oxidation in the course of two-dimensional PAGE and in-gel digestion. The latter suggestion is also supported by the fact that Prx II isolated from aged erythrocytes was in the sulfinic acid oxidation state (25).

Other 2-Cys Prx enzymes are as sensitive to hyperoxidation as Prx I (29, 41). What might be the significance of Prx inactivation during catalysis? Apoptosis is one realm in which such inactivation could assume a regulatory role. Prx enzymes have been shown to protect various cell types from apoptosis induced by exogenous factors such as cytokines, serum deprivation, ceramide, H_2O_2, UV irradiation, and certain cancer drugs (42, 43). These diverse stimuli trigger the production of reactive oxygen species that damage lipids, protein, and DNA, eliciting apoptosis as a consequence. Hyperoxidized Prx accumulates at the expense of active Prx as seen in H_2O_2-treated cells (Fig. 6). Accumulation of hyperoxidized Prx enzymes has also been shown in tumor necrosis factor-α-treated cells (41). Meanwhile, the turnover rate of Prx enzymes in H_2O_2-treated cells remains as slow as that in untreated cells.[2] Thus, oxidation-mediated inactivation of Prx enzymes would inevitably disrupt the balance of production and elimination of H_2O_2, leading to H_2O_2 accumulation. Enzyme inactivation proceeds in proportion to the number of catalytic cycles, and inactivated enzyme molecules would accumulate once the inactivation rate crosses a certain threshold. Thus, the fraction of inactive Prx molecules could serve as a record of the cell's history of exposure to oxidative stress. Cells that are subjected to prolonged oxidative stress are likely to suffer irreparable damage, necessitating programmed cell death. One speculation is that accumulation of hyperoxidized Prx enzymes at the expense of active enzyme molecules and the resulting accumulation of H_2O_2 might trigger damage-induced programmed cell death when integrated with other cellular signals. This hypothesis obviously demands many more studies, including those addressing the fate of inactivated Prx enzymes.

[2] H. Z. Chae, S. C. Hwang, and S. G. Rhee, unpublished data.

REFERENCES

1. Chae, H. Z., Chung, S. J., and Rhee, S. G. (1994) *J. Biol. Chem.* **269,** 27670–27678
2. Rhee, S. G., Kang, S. W., Chang, T. S., Jeong, W., and Kim, K. (2001) *International Union of Biochemistry and Molecular Biology Life* **52,** 35–41
3. Hofmann, B., Hecht, H. J., and Flohé, L. (2002) *Biol. Chem. Hoppe-Seyler* **383,** 347–364
4. Kim, K., Kim, I. H., Lee, K. Y., Rhee, S. G., and Stadtman, E. R. (1988) *J. Biol. Chem.* **263,** 4704–4711
5. Kim, I. H., Kim, K., and Rhee, S. G. (1989) *Proc. Natl. Acad. Sci. U. S. A.* **86,** 6018–6022
6. Chae, H. Z., Kim, I. H., Kim, K., and Rhee, S. G. (1993) *J. Biol. Chem.* **268,** 16815–16821
7. Tartaglia, L. A., Storz, G., and Ames, B. N. (1989) *J. Mol. Biol.* **210,** 709–719
8. Storz, G., Jacobson, F. S., Tartaglia, L. A., Morgan, R. W., Silveira, L. A., and Ames, B. N. (1989) *J. Bacteriol.* **171,** 2049–2055
9. Tartaglia, L. A., Storz, G., Brodsky, M. H., Lai, A., and Ames, B. N. (1990) *J. Biol. Chem.* **265,** 10535–10540
10. Chae, H. Z., Robison, K., Poole, L. B., Church, G., Storz, G., and Rhee, S. G. (1994) *Proc. Natl. Acad. Sci. U. S. A.* **91,** 7017–7021
11. Chae, H. Z., and Rhee, S. G. (1994) *Biofactors* **4,** 177–180
12. Matsumoto, A., Okado, A., Fujii, T., Fujii, J., Egashira, M., Niikawa, N., and Taniguchi, N. (1999) *FEBS Lett.* **443,** 246–250
13. Seo, M. S., Kang, S. W., Kim, K., Baines, I. C., Lee, T. H., and Rhee, S. G. (2000) *J. Biol. Chem.* **275,** 20346–20354
14. Chae, H. Z., Uhm, T. B., and Rhee, S. G. (1994) *Proc. Natl. Acad. Sci. U. S. A.* **91,** 7022–7026
15. Kang, S. W., Chae, H. Z., Seo, M. S., Kim, K., Baines, I. C., and Rhee, S. G. (1998) *J. Biol. Chem.* **273,** 6297–6302
16. Jin, D. Y., Chae, H. Z., Rhee, S. G., and Jeang, K. T. (1997) *J. Biol. Chem.* **272,** 30952–30961
17. Jacobson, F. S., Morgan, R. W., Christman, M. F., and Ames, B. N. (1989) *J. Biol. Chem.* **264,** 1488–1496
18. Kang, S. W., Baines, I. C., and Rhee, S. G. (1998) *J. Biol. Chem.* **273,** 6303–6311
19. Choi, H. J., Kang, S. W., Yang, C. H., Rhee, S. G., and Ryu, S. E. (1998) *Nat. Struct. Biol.* **5,** 400–406
20. Fujii, T., Fujii, J., and Taniguchi, N. (2001) *Eur. J. Biochem.* **268,** 218–225
21. Fisher, A. B., Dodia, C., Manevich, Y., Chen, J. W., and Feinstein, S. I. (1999) *J. Biol. Chem.* **274,** 21326–21334
22. Singh, A. K., and Shichi, H. (1998) *J. Biol. Chem.* **273,** 26171–26178
23. Peshenko, I. V., Novoselov, V. I., Evdokimov, V. A., Nikolaev, Y. V., Kamzalov, S. S., Shuvaeva, T. M., Lipkin, V. M., and Fesenko, E. E. (1998) *Free Radic. Biol. Med.* **25,** 654–659
24. Hirotsu, S., Abe, Y., Okada, K., Nagahara, N., Hori, H., Nishino, T., and Hakoshima, T. (1999) *Proc. Natl. Acad. Sci. U. S. A.* **96,** 12333–12338
25. Schröder, E., Littlechild, J. A., Lebedev, A. A., Errington, N., Vagin, A. A., and Isupov, M. N. (2000) *Struct. Fold. Des.* **8,** 605–615
26. Alphey, M. S., Bond, C. S., Tetaud, E., Fairlamb, A. H., and Hunter, W. N. (2000) *J. Mol. Biol.* **300,** 903–916
27. Wood, Z. A., Poole, L. B., Hantgan, R. R., and Karplus, P. A. (2002) *Biochemistry* **41,** 5493–5504
28. Kim, J. R., Yoon, H. W., Kwon, K. S., Lee, S. R., and Rhee, S. G. (2000) *Anal. Biochem.* **283,** 214–221
29. Mitsumoto, A., Takanezawa, Y., Okawa, K., Iwamatsu, A., and Nakagawa, Y. (2001) *Free Radic. Biol. Med.* **30,** 625–635
30. Chae, H. Z., Kang, S. W., and Rhee, S. G. (1999) *Methods Enzymol.* **300,** 219–226
31. Chae, H. Z., Kim, H. J., Kang, S. W., and Rhee, S. G. (1999) *Diabetes Res. Clin. Pract.* **45,** 101–112
32. Poole, L. B., and Claiborne, A. (1989) *J. Biol. Chem.* **264,** 12330–12338
33. Ellis, H. R., and Poole, L. B. (1997) *Biochemistry* **36,** 13349–13356
34. Montemartini, M., Kalisz, H. M., Hecht, H. J., Steinert, P., and Flohé, L. (1999) *Eur. J. Biochem.* **264,** 516–524
35. Allison, W. S. (1976) *Acc. Chem. Res.* **9,** 293–299
36. Davis, F. A., Jenkins, L. A., and Billmers, R. L. (1986) *J. Org. Chem.* **51,** 1033–1040
37. Claiborne, A., Yeh, J. I., Mallett, T. C., Luba, J., Crane, E. J., III, Charrier, V., and Parsonage, D. (1999) *Biochemistry* **38,** 15407–15416
38. Yeh, J. I., Claiborne, A., and Hol, W. G. (1996) *Biochemistry* **35,** 9951–9957
39. Crane, E. J., III, Yeh, J. I., Luba, J., and Claiborne, A. (2000) *Biochemistry* **39,** 10353–10364
40. Flohé, L., Budde, H., Bruns, K., Castro, H., Clos, J., Hofmann, B., Kansal-Kalavar, S., Krumme, D., Menge, U., Plank-Schumacher, K., Sztajer, H., Wissing, J., Wylegalla, C., and Hecht, H. J. (2002) *Arch. Biochem. Biophys.* **397,** 324–335
41. Rabilloud, T., Heller, M., Gasnier, F., Luche, S., Rey, C., Aebersold, R., Benahmed, M., Louisot, P., and Lunardi, J. (2002) *J. Biol. Chem.* **277,** 19396–19401
42. Zhang, P., Liu, B., Kang, S. W., Seo, M. S., Rhee, S. G., and Obeid, L. M. (1997) *J. Biol. Chem.* **272,** 30615–30618
43. Shen, C., and Nathan, C. (2002) *Mol. Med.* **8,** 95–102
44. Gay, C. A., and Gebicki, J. M. (2002) *Anal. Biochem.* **304,** 42–46

Inactivation of Human Peroxiredoxin I during Catalysis as the Result of the Oxidation of the Catalytic Site Cysteine to Cysteine-sulfinic Acid

Kap-Seok Yang, Sang Won Kang, Hyun Ae Woo, Sung Chul Hwang, Ho Zoon Chae, Kanghwa Kim and Sue Goo Rhee

J. Biol. Chem. 2002, 277:38029-38036.
doi: 10.1074/jbc.M206626200 originally published online August 2, 2002
